Particle tracking for time-fractional diffusion

Yong Zhang*
Desert Research Institute, Las Vegas, Nevada 89119, USA

Mark M. Meerschaert†
Department of Statistics and Probability, Michigan State University, East Lansing, Michigan 48824, USA

Boris Baeumer‡
Department of Mathematics and Statistics, University of Otago, Dunedin 9054, New Zealand

(Received 16 July 2008; published 19 September 2008)

A particle tracking code is developed to solve a general time-fractional diffusion equation (FDE), yielding a Lagrangian framework that can track particle dynamics. Extensive simulations demonstrate the efficiency and flexibility of this simple Langevin approach. Many real problems require a vector FDE with variable parameters and multiscaling spreading rates. For these problems, particle tracking is the only viable solution method.

DOI: 10.1103/PhysRevE.78.036705 PACS number(s): 02.60.Cb, 05.40.Fb, 05.10.Gg

I. INTRODUCTION

Fractional diffusion equations extend the classical model, substituting fractional derivatives for their integer-order analog. Fractional derivatives in space model anomalous superdiffusion, driven by large particle jumps. Fractional derivatives in time can capture anomalous subdiffusion, related to long waiting times between particle jumps [1] (see further discussion in the next section). In practice, a combination of subdiffusive and superdiffusive effects can manifest in the same problem. A contaminant undergoing natural gradient flow through a porous medium may exhibit early arrival downstream (superdiffusion) as well as slow concentration decay at late times (subdiffusion). In addition, a physically realistic model requires consideration of multiple spatial dimensions, the possibility of correlation between motion in each coordinate, and the likelihood of variations in the porous medium structure [2,3]. All of these factors present serious challenges for Eulerian simulation codes.

Numerical methods for fractional diffusion equations (FDEs) have been the focus of many recent studies due to the prevalence of anomalous diffusion processes in nature [4–6] and the impossibility of exact analytical solutions for most fractional partial differential equations. Many successful methods are Eulerian: finite difference methods [7–17]; the finite element method [18–22]; the method of lines [23–25]; and the mixed Lagrangian-Eulerian method [26,27].

Unlike Eulerian solvers, particle-tracking yields a grid-free, fully Lagrangian solution by simulating sample paths of the underlying stochastic process [28–32]. To simulate the macroscopic transport, random walker (or particle) locations are updated based on local velocity and/or dispersion strength, combined with a random trapping time (see also the excellent reviews of the particle tracking approach and the extensive references cited by Delay *et al.* [28] and Salamon *et al.* [32]). In particular, Dentz *et al.* [33] approximated the generalized master equation with a temporal memory kernel using a discrete particle tracking routine [expressed by their equations (13) and (14)], where the spatial and temporal random increments (which are independent) for each particle are generated according to the predefined probability density functions (PDFs) for jump size and waiting time, respectively. A similar particle tracking routine was also described briefly by Berkowitz and Scher [34]. Note the above two references assume instantaneous particle jumps, which requires more time steps than the Lagrangian scheme developed in this study (where the particle has a finite velocity while motionless for extended periods of time).

Particle tracking increases computational efficiency for large-scale flow systems with fine mesh [35,36] and overcomes the grid-average error for simulating a sharp density front [37,38]. These advantages of the Lagrangian solver have motivated the recent development of particle-based approximations for the FDE. Chechkin *et al.* [39] and Zhang *et al.* [40] approximate the space-fractional FDE using a Langevin approach. Marseguerra and Zoia [30,31,41] develop a Monte Carlo approach to model subdiffusion across a discontinuity of parameters. Heinsalu *et al.* [42] develop a continuous time random walk scheme for the time fractional Fokker-Planck equation (FFPE). Magdziarz and Weron [43] develop a robust Monte Carlo approach to solve the one-dimensional (1D) spatiotemporal FFPE.

This study proposes a particle tracking method for the time-fractional diffusion equation. It is a logical extension of Zhang *et al.*'s [40] Lagrangian solver, which treats the space-fractional FDE. The methodology is developed in the next section. In Sec. III, we report on the results of extensive simulation studies. This includes a comparison with other numerical solutions, when available, and model fitting to field data, for which no other simulation methods are available. Conclusions are drawn in Sec. IV.

II. TIME-LANGEVIN APPROACH AND THE RESULTANT LAGRANGIAN FRAMEWORK

The FDE considered in this study has a general form,

*yong.zhang@dri.edu
†mcubed@stt.msu.edu
‡bbaeumer@maths.otago.ac.nz

$$\left(b\frac{\partial}{\partial t}+\beta\frac{\partial^{\gamma}}{\partial t^{\gamma}}\right)p(x,t)=A_x p(x,t)+\beta\frac{t^{-\gamma}}{\Gamma(1-\gamma)}p_0(x), \quad (1)$$

where $p(x,t)$ is a PDF representing the relative concentration of moving particles with initial condition $p(x,t=0)=p_0(x)$; $0<\gamma<1$ is the order of the Riemann-Liouville fractional time derivative; $b\geqslant 0$ and $\beta\geqslant 0$ are arbitrary parameters; and A_x denotes the advection-diffusion operator. If $b=1$, Eq. (1) reduces to the fractal mobile and immobile transport model proposed by Schumer *et al.* [44]. If $b=0$ and $\beta=1$, Eq. (1) reduces to the fractional kinetic equation of Zaslavsky [45]. The general equation (1) governs a subordinated process $W(E_t)$, where the transition density of $W(t)$ is the Green's function solution of $\partial u/\partial t=A_x u$, and $\tau=E_t$ is the inverse or first passage time for the process $t=b\tau+\beta D_\tau$, with D_τ a classical stable subordinator of index γ, compare [46]. The outer process $W(\tau)$ models the location of a moving particle, and the subordinator adjusts for resting time that intervenes, due to sticking or trapping. While the treatment here is completely general, in practical applications we take $b=1$ or $b=0$.

It is also noteworthy that the time fractional derivative in Eq. (1) does not produce pure subdiffusion if the motion operator A_x includes an advective component. For example, when $b=0$, $\beta=1$, and $A_x=-v\partial/\partial x+D\partial^2/\partial x^2$ (where v and D denote the velocity and dispersion coefficient, respectively), the corresponding mean squared displacement is [see Eqs. (39) and (92) in Metzler and Klafter [4] and Eq. (2c) in Zhang *et al.* [47]]

$$\langle x^2(t)\rangle=\frac{2}{\Gamma(\gamma+1)}Dt^{\gamma}+\left[\frac{2}{\Gamma(2\gamma+1)}-\frac{1}{\Gamma(\gamma+1)^2}\right]v^2t^{2\gamma},$$

which spreads faster than the classical diffusion rate $\langle x^2(t)\rangle=\sigma^2 t$ if $0.5<\gamma<1$.

The function p in Eq. (1) is a density of random walkers with decoupled jump sizes and waiting times. It can be calculated by subordinating the jump process against the waiting time process (see [1] or [46, Theorem 4.1]):

$$p(x,t)=\int_0^{\infty}u(x,\tau)h(\tau,t)d\tau, \quad (2)$$

where t denotes clock time, and τ denotes operational time. The first density $u(x,\tau)$ on the right-hand side (rhs) models particle motion in operational time τ:

$$\frac{\partial}{\partial\tau}u(x,\tau)=A_x u(x,\tau) \quad (3)$$

with initial condition $u(x,\tau=0)=p_0(x)$. The second density $h(\tau,t)$ on the rhs of Eq. (2) adjusts the particle motion to allow for long waiting times, and is governed by

$$\frac{\partial}{\partial\tau}h(\tau,t)=-\left[b\frac{\partial h(\tau,t)}{\partial t}+\beta\frac{\partial^{\gamma}h(\tau,t)}{\partial t^{\gamma}}\right] \quad (4)$$

with initial condition $h(\tau=0,t)=b\delta(t)+\beta t^{-\gamma}/\Gamma(1-\gamma)$. It contains a drift term and a diffusion component in clock time t, analogous to the advection and diffusion in space. The translation from operational to clock time accounts for the effect of the fractional time derivative [1,48]. Note that fractional dynamics is often understood in terms of Bochner's subordination principle [49,50], which links the operational time and the physical clock time (for example, see applications by Yuste and Lindenberg [51], Sokolov and Metzler [52], Magdziarz and Weron [43], Baeumer and Meerschaert [53], among many others). The numerical transfer from operational time to clock time, as outlined in the following, is much easier than its inverse subordination process.

The forward-in-time equation (4) needs to be converted to its backward-in-time counterpart to build the Langevin equation. Let $H(s,t)$ be the hitting time density of the backward time $s=\tau_{end}-\tau$, where τ_{end} is the final forward time ($\tau_{end}\geqslant\tau$). Following the argument in [40], we obtain the backward equation

$$\frac{\partial}{\partial s}H(s,t)=b\frac{\partial H(s,t)}{\partial t}-\beta\frac{\partial^{\gamma}H(s,t)}{\partial(-t)^{\gamma}} \quad (5)$$

for the Markov process

$$dT=bd\tau+dw, \quad (6)$$

where the stable random noise

$$dw=\left[\left|\beta\cos\frac{\pi\gamma}{2}\right|d\tau\right]^{1/\gamma}S_{\gamma}(\beta^*=+1,\sigma^*=1,\mu=0), \quad (7)$$

and $S_\gamma(+1,1,0)$ is a standard stable random variable in the Samorodnitsky and Taqqu [54] parametrization (with β^*, σ^*, and μ denoting the skewness, scale, and shift, respectively). Equation (7) provides the sample path of the hitting time process (4).

The Lagrangian framework to approximate (1) requires three steps [46,55,56].

Step 1. Transform operational time τ to the corresponding clock time t, based on Eq. (6). $d\tau$ is the predefined operational time step, and the noise dw is then calculated using Eq. (7).

Step 2. Simulate the particle jump dX during operational time step $d\tau$. Note that the particle motion process $X(\tau)$ is Markovian. Examples will be shown in the next section.

Step 3. Calculate the particle location at each clock time grid t_i using

$$Y(t_i)=X(\tau_i)=X\left(\sum_{j=1}^{i}(d\tau)_j\right), \quad (8)$$

where τ_i is the operational time corresponding to clock time t_i.

By repeating these three steps until the modeling time exceeds the target clock time T_{end} (i.e., $\Sigma dt\geqslant T_{end}$), we obtain the solution $p(x,t)$ of Eq. (1) up to time T_{end}. The algorithm outputs the solution p at *irregular* time grids t_i due to the random noise dw. It is straightforward to interpolate t to get a regular output, as in [43].

III. NUMERICAL EXAMPLES

The Lagrangian solver developed in Sec. II is tested against other numerical solutions and fit to field measure-

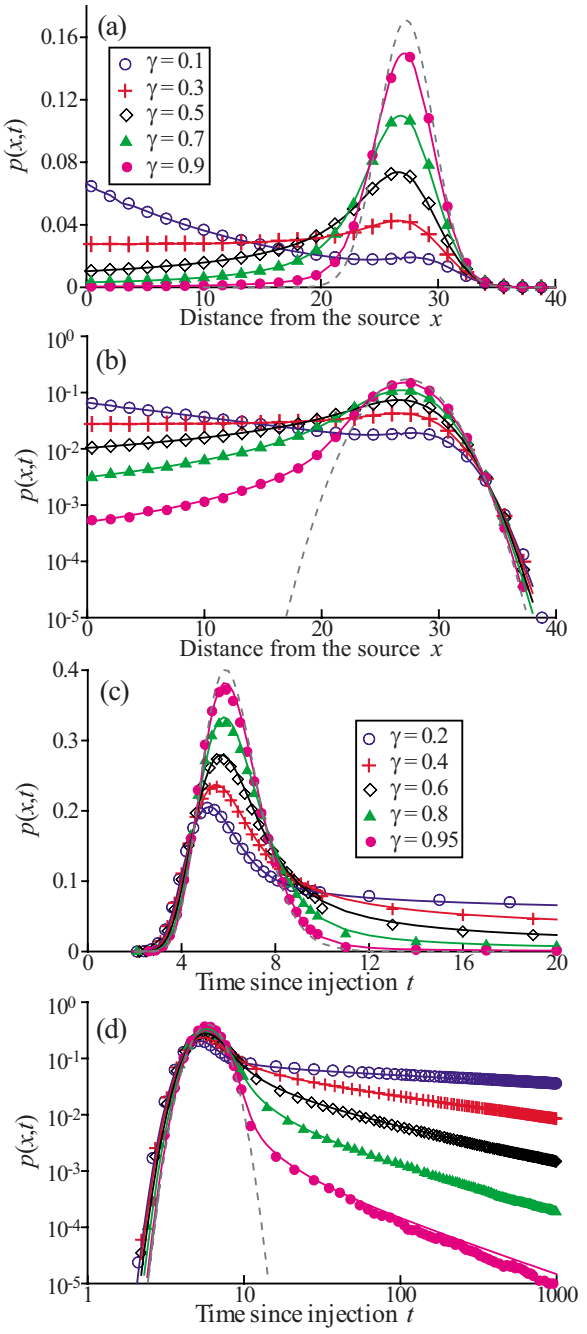

FIG. 1. (Color online) Lagrangian approximation (symbols) of Eq. (1) with $b=1$ and operator (9) vs the semianalytical solution (lines) developed by Schumer *et al.* [44]. The time scale index γ varies from 0 to 1, while the space scale index α is limited to 2. The classical second-order advection-diffusion equation $\partial p/\partial t = -v\partial c/\partial x + D\partial^2 C/\partial x^2$ is also shown (dashed line) for comparison. (a) The spatial distribution of $p(x,t)$, with parameters $v=1$, $D=0.1$, $t=30$, $\gamma=0.1-0.9$, $\beta=0.1$, and the instantaneous source at $x=0$. (c) The temporal evolution of $p(x,t)$, with $v=1$, $D=0.1$, $\gamma=0.2-0.95$, $\beta=0.2$, the initial source at $x=0$, and the control plane at distance 5. (b) The semilog plot of (a), and (d) the log-log plot of (c).

ments in cases where no other solution is available. To check the full capability of the Lagrangian solver, different advection-diffusion operators A_x are selected. The three-step Lagrangian framework is used for all examples. In the second step, the particle jump size dX depends on the form of A_x.

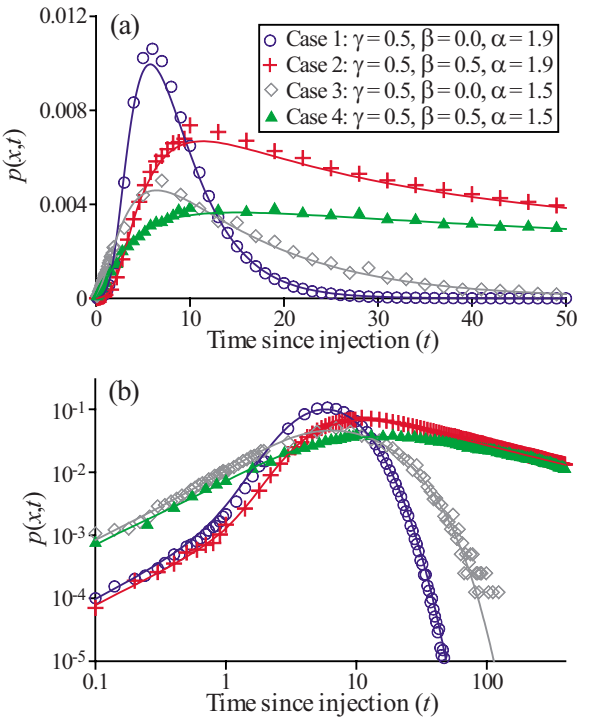

FIG. 2. (Color online) Lagrangian approximations (symbols) of Eq. (1) with $b=1$ and operator (9) vs the implicit Eulerian solutions after time-subordination operation (lines), for four different cases. Some parameters are the same in all cases, including: $v(x)=2+0.04x$, $D(x)=8+0.15x$, $\gamma=0.5$, an instantaneous source at $x=50$, and the control plane at distance 80. (b) The log-log plot of (a).

A. Spatiotemporal fractional diffusion equation

If the advection-diffusion operator A_x in Eq. (1) is

$$A_x = -\frac{\partial}{\partial x}v(x) + \frac{\partial^{\alpha-1}}{\partial x^{\alpha-1}}\left[D(x)\frac{\partial}{\partial x}\right], \tag{9}$$

then Eq. (1) is a space and time FDE with variable velocity v and diffusion coefficient D. Here $1<\alpha\leqslant 2$ is the order of the space fractional derivative.

The jump size dX at each time step $d\tau$ is approximated by the space-Langevin equation [40]

$$dX = v\,d\tau + B_1 S_\alpha(+1,1,0) + B_2 S^*_{\alpha-1}(+1,1,0), \tag{10}$$

where

$$B_1 = \left[\left(-\cos\frac{\pi\alpha}{2}\right)Dd\tau\right]^{1/\alpha},$$

$$B_2 = \mathrm{sign}\left(\frac{\partial D}{\partial x}\right)\left|\cos\left(\frac{\pi(\alpha-1)}{2}\right)\frac{\partial D}{\partial x}d\tau\right|^{1/(\alpha-1)},$$

and the two random noises S and S^* are independent. If $D(x)$ is a constant, then $B_2=0$, and Eq. (10) is similar to the time

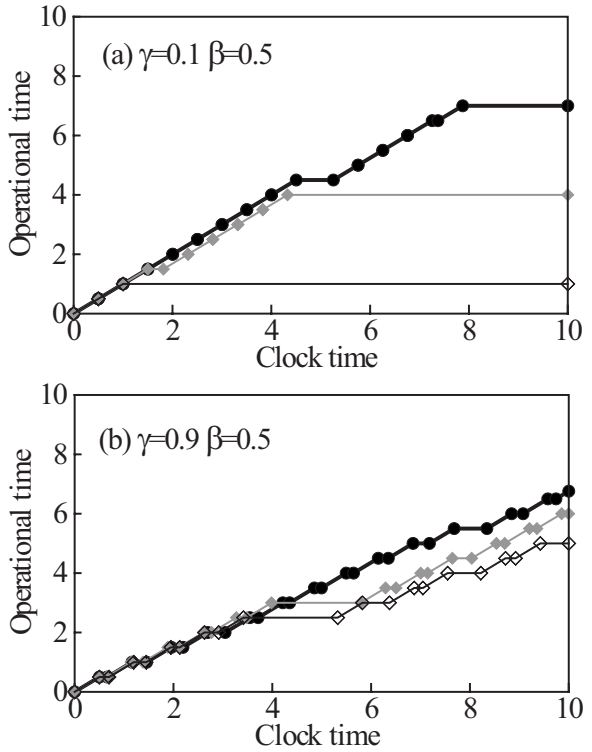

FIG. 3. Operational time vs clock time. Different lines represent a different sample path in time.

Langevin equation (6).

Extensive tests of this Lagrangian framework have been performed, with a few examples shown in Fig. 1 and 2. The Lagrangian results generally match the semianalytical solutions for various γ (Fig. 1). When parameters v and D vary in space, there is no semianalytical solution, and we then check the Lagrangian solution using the implicit Eulerian solution [40] with numerical time-subordination transform. Note the implicit Eulerian scheme developed by Zhang *et al.* [40] is unconditionally stable. The Lagrangian solutions generally match the Eulerian solutions (Fig. 2).

Note the first step of the Lagrangian framework, expressed by Eq. (6), efficiently converts operational time to clock time (see Fig. 3 for examples) using the inverse process of $h(\tau,t)$. In this case $b=1$, one can interpret operational time as the mobile time of a particle undergoing advection and dispersion while simultaneously transitioning between two phases: mobile and immobile. The first term of Eq. (6) is the mobile time $d\tau$, and the second term is the random immobile waiting time dw that accumulates during mobile time $d\tau$, so that $dt=d\tau+dw$ is the clock time [48].

Other forms of the space fractional diffusion in Eq. (9) are possible, resulting in a jump size dX different from Eq. (10), while the time-Langevin equation (6) remains unchanged. For example, if the net diffusive flux in Eq. (9) is replaced by $\frac{\partial}{\partial x}[D(x)\frac{\partial^{\alpha-1}}{\partial x^{\alpha-1}}]$ and $D(x)$ varies linearly, then the parameter B_2 in Eq. (10) needs to be rescaled by $(\alpha-1)^{1/(\alpha-1)}$ [40]. If the net diffusive flux in Eq. (9) takes the form of $\frac{\partial^{\alpha}}{\partial x^{\alpha}}D(x)$, then the FDE (1) reduces to the FFPE with position-dependent parameters proposed by Srokowski and Kaminska [57] [see their Eq. (14)], and the corresponding Markov process contains only the first two terms on the rhs of Eq. (10). Numerical examples (not shown here) validate these conclusions.

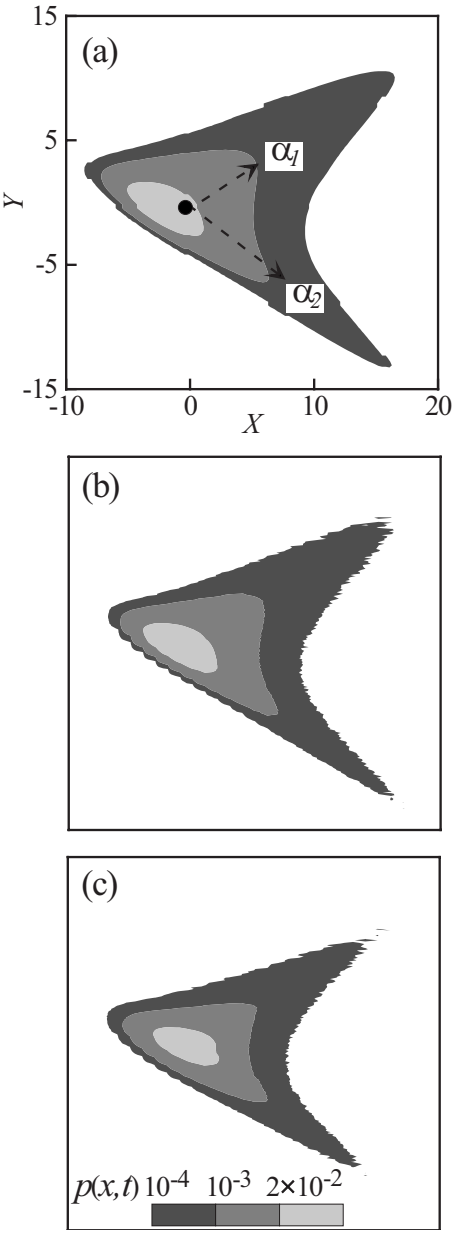

FIG. 4. The 2D density described by Eq. (11) with $b=1$ at time $t=1$ with $v=0$, $D_1=D_2=1$, $\alpha_1=1.3$, and $\alpha_2=1.7$. The mixing measure is assigned along two discrete directions: $M_1=M(30°)=0.4$, $M_2=M(-35°)=0.6$. (a) Semianalytical solution with $\beta=0$. (b) Lagrangian solution with $\gamma=0.98$ and $\beta=0.5$. (c) Lagrangian solution with $\gamma=0.3$ and $\beta=0.2$. The circle (exaggerated for display) in (a) denotes the particle source location (0,0) at time 0.

B. FDE with direction-dependent spreading rate in space

If the time FDE contains direction-dependent scaling rates, the model (1) extends to

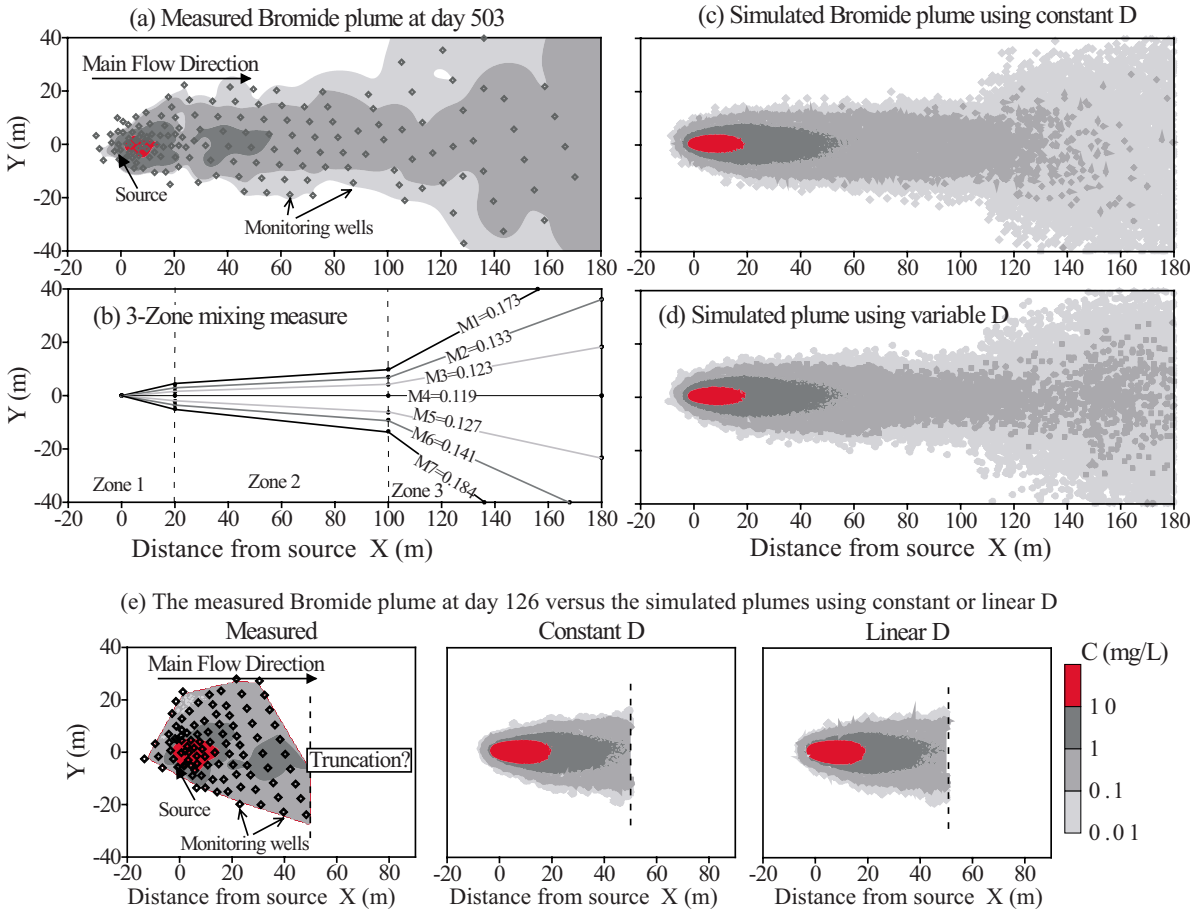

FIG. 5. (Color online) The measured Bromide plumes at days 503 (a) and 126 (e) vs the simulated plumes [(c)–(e)] using the FDE (11). The parameters (either predicted or fitted) are the space scale index $\alpha_x=1.1$, $\alpha_y=1.5$, time index $\gamma=0.35$, coefficient $\beta=0.08$ days$^{-0.65}$, $v_x=0.30$ m/day, $v_y=0$, and $D_y=0.30$ m$^{1.5}$/day. (a) The measured plume at day 503. (b) The best-fit three-zone mixing measure with seven discrete directions and weights. (c) The simulated plume at day 503 using constant D_x ($D_x=0.30$ m$^{1.1}$/day). (d) The simulated plume at day 503 using space-dependent D_x ($D_x=0.30+0.0017x$ m$^{1.1}$/day). (e) The measured plume at day 126 vs the simulated plumes using constant or linear D_x. In (e), the simulated plume using the constant D_x is similar to that with linear D_x, due to the truncation of plumes. The diamonds in (a) and (e) denote the locations of samplers at the MADE site.

$$b\frac{\partial}{\partial t}[p(\vec{x},t)] + \beta\frac{\partial^{\gamma}}{\partial t^{\gamma}}[p(\vec{x},t)] = -\nabla_M^{\boldsymbol{H}^{-1}}\cdot[\mathbf{v}(\vec{x})p(\vec{x},t) - D(\vec{x})\nabla p(\vec{x},t)] + \beta\frac{t^{-\gamma}}{\Gamma(1-\gamma)}p_0(\vec{x}), \quad (11)$$

with initial condition $p(\vec{x},t=0)=p_0(\vec{x})$, where $\boldsymbol{H}^{-1}$ is the inverse of the scaling matrix providing the order and direction of the fractional derivatives, and $M=M(d\theta)$ is the mixing measure [2,58]. The mixing measure defines the shape and skewness of the density in multidimensions by assigning the probability of particle jumps in the angular sector $d\theta$ (denoted as $\vec{\theta}_i$ in the following equation, and can be either continuous or discrete) [see Fig. 5(b) for a space-dependent mixing measure]. The eigenvalues of matrix $\boldsymbol{H}$ are the Hurst index coefficients $1/\alpha$ of the growth process. For a 3D case, if the primary directions of growth are perpendicular, the scaling terms in each of the principal directions $1/\alpha_j$ are the eigenvalues of matrix $\boldsymbol{H}$, which is of the form

$$\boldsymbol{H}_0 = \begin{bmatrix} 1/\alpha_x & 0 & 0 \\ 0 & 1/\alpha_y & 0 \\ 0 & 0 & 1/\alpha_z \end{bmatrix}$$

(see also Schumer *et al.* [44]).

Particle jumps follow a multiscaling compound Poisson process [58]

$$\vec{Z}(\tau) = \sum_{i=1}^{N}\vec{X}_i = \sum_{i=1}^{N} R_i^{\boldsymbol{H}}\vec{\theta}_i, \quad (12)$$

where $\vec{Z}(\tau)$ represents the particle location at operational time τ, N is the number of random jumps by time τ, and the jump direction $\vec{\theta}_i$ is a random unit vector drawn from the CDF of the mixing measure $M=M(d\theta)$. Eigenvalues of the matrix $\boldsymbol{H}$ control the jump sizes in each eigenvector coordinate. The jump component of $R^{\boldsymbol{H}}$ along the eigenvector belonging to the kth eigenvalue $1/\alpha_k$ of $\boldsymbol{H}$ depends on the space-dependent parameters $\mathbf{v}$ and D [58]:

$$R_i^{1/\alpha_k} = v(X_k)d\tau + B_1(X_k)S_\alpha + B_2(X_k)S^*_{\alpha-1},$$

where k represents the direction of the kth eigenvector of $\boldsymbol{H}$.

One example is shown in Fig. 4. A 2D density described by Eq. (11) with $\beta=0$ is solved using the semianalytical approach [44] [Fig. 4(a)]. Zhang *et al.* [58] showed that the model (11) with $\beta=0$ (i.e., the space-only fractional diffusion model) can be approximated successfully using Eq. (12). For the case of combined sub- and super-diffusion, the semi-analytical approach is no longer efficient, while the Langevin-based Lagrangian solver developed in this study is even more computationally efficient (since fewer jumps are required). With an increased coefficient β [Fig. 4(b)] and/or a decreased index γ [Fig. 4(c)], the leading edge of density p shrinks, as expected.

Field applications, such as the prediction of contaminant transport in natural heterogeneous media, require a multiple dimensional model beyond any 1D simplification. For example, the Bromide plumes observed at the MADE site in Columbus, MS, which perhaps is the best-studied and most representative heterogeneous site in North America [59–62], are anomalous with direction-dependent (superdiffusive) spreading rates, irregular channeling of the plume front along preferential flow paths, solute retention (subdiffusion) by a relatively immobile phase, and local variation of transport speed possibly due to nonstationary heterogeneity. These Bromide plumes have attracted continuing interest and motivated the development of transport theories in the hydrology community in the last 15 years, but a reliable numerical model has never been built (see the recent review of Molz *et al.* [63]). Our preliminary tests show that the FDE (11) with a space-dependent mixing measure and constant $\mathbf{v}$ and D can capture the fan shape of the measured plume, but misses the heavy leading edge at late-time sampling cycles. We then allow D to vary in space (see parameters in Fig. 5) to represent successfully the observed spatial variation of deposits and to get a better fit of the observed leading plume front. Figures 5(d) and 5(e) show the high-dimensional, numerical simulation that can capture all anomalous behaviors of MADE-site Bromide plumes. It is noteworthy that the multidimensional Lagrangian solver developed in this section is not only efficient, but also the only available tool for the applicable FDE model (11).

IV. CONCLUSIONS

The stochastic model underlying the time-fractional diffusion equation can be separated into a motion process and an independent operational time process. The operational time process embedded in the FDE model contains a linear motion portion and a stable random noise with index γ. The Langevin equation can be constructed for each process to track particle evolution in space and time. A Lagrangian scheme with independent particle jumps and waiting times can then be developed by combining the two Langevin equations to solve the space-time fractional FDE in one or multiple dimensions. The core of the particle tracking model is the numerical conversion of operational time to clock time using a time-domain Langevin approach, which greatly simplifies simulation of the non-Markovian particle motion.

Particle tracking solutions of the space-time fractional FDE generally match solutions obtained from semianalytical or Eulerian methods. The space-time FDE model in multiple dimensions with variable coefficients yields a reasonable model for the complex and well-studied MADE-site Bromide plumes. Numerical examples and field application show the applicability, efficiency, and flexibility of the Lagrangian solver developed in this study.

ACKNOWLEDGMENTS

The work was supported by the National Science Foundation under Grants No. EAR-0748953 and No. DMS-0706440. We would like to thank the anonymous reviewers of this paper for their excellent comments and suggestions to revise and enhance portions of this paper.

[1] M. M. Meerschaert, D. A. Benson, H.-P. Scheffler, and B. Baeumer, Phys. Rev. E **65**, 041103 (2002).
[2] M. M. Meerschaert, D. A. Benson, and B. Baeumer, Phys. Rev. E **63**, 021112 (2001).
[3] Y. Zhang, D. A. Benson, M. M. Meerschaert, and E. M. LaBolle, Water Resour. Res. **43**, W05439 (2007).
[4] R. Metzler and J. Klafter, Phys. Rep. **339**, 1 (2000).
[5] R. Metzler and J. Klafter, J. Phys. A **37**, R161 (2004).
[6] R. Metzler, A. V. Chechkin, and J. Klafter, *Encyclopaedia of Complexity and System Science*, edited by Henrik Jeldtoft Jensen (Springer-Verlag, Berlin, 2007).
[7] C. M. Chen, F. Liu, I. Turner, and V. Anh, J. Comput. Phys. **227**, 886 (2007).
[8] C. M. Chen, F. Liu, and K. Burrage, Appl. Math. Comput. **198**, 754 (2008).
[9] Z.-Q. Deng, V. P. Singh, and L. Bengtsson, J. Hydraul. Eng. **130**, 422 (2004).
[10] T. A. M. Langlands and B. I. Henry, J. Comput. Phys. **205**, 719 (2005).
[11] F. Liu, P. Zhuang, V. Anh, I. Turner, and K. Burrage, Appl. Math. Comput. **191**, 12 (2007).
[12] V. E. Lynch, B. A. Carreras, D. del-Castillo-Negrete, K. M. Ferreira-Mejias, and H. R. Hicks, J. Comput. Phys. **192**, 406 (2003).
[13] M. M. Meerschaert and C. Tadjeran, J. Comput. Appl. Math. **172**, 65 (2004).
[14] Z. Z. Sun and X. N. Wu, Appl. Numer. Math. **56**, 193 (2006).
[15] C. Tadjeran and M. M. Meerschaert, J. Comput. Phys. **213**, 205 (2006).
[16] S. B. Yuste and L. Acedo, SIAM (Soc. Ind. Appl. Math.) J. Numer. Anal. **42**, 1862 (2005).
[17] S. B. Yuste, J. Comput. Phys. **216**, 264 (2006).
[18] V. J. Ervin, N. Heuer, and J. P. Roop, SIAM (Soc. Ind. Appl. Math.) J. Numer. Anal. **45**, 572 (2007).

[19] V. J. Ervin and J. P. Roop, Numer. Methods Partial Differ. Equ. **23**, 256 (2007).
[20] V. J. Ervin and J. P. Roop, Numer. Methods Partial Differ. Equ. **22**, 558 (2006).
[21] G. J. Fix and J. P. Roop, Comput. Math. Appl. **48**, 1017 (2004).
[22] J. P. Roop, J. Comput. Appl. Math. **193**, 243 (2006).
[23] W. H. Deng, J. Comput. Phys. **227**, 1510 (2007).
[24] F. Liu, V. Anh, and I. Turner, J. Comput. Appl. Math. **166**, 209 (2004).
[25] F. Liu, V. Anh, I. Turner, and P. Zhuang, Aust N. Z. Ind. Appl. Math. J. **45(E)**, C461 (2004).
[26] R. Gorenflo, F. Mainardi, D. Moretti, and P. Paradisi, Nonlinear Dyn. **29**, 129 (2002).
[27] R. Gorenflo, A. Vivoli, and F. Mainardi, Nonlinear Dyn. **38**, 101 (2004).
[28] F. Delay, P. Ackerer, and C. Danquigny, Vadose Zone J. **4**, 360 (2005).
[29] A. E. Hassan and M. M. Mohamed, J. Hydrol. **275**, 242 (2002).
[30] M. Marseguerra and A. Zoia, Ann. Nucl. Energy **33**, 223 (2006).
[31] M. Marseguerra and A. Zoia, Physica A **377**, 448 (2007).
[32] P. Salamon, D. Fernàndez-Gareia, and J. J. Gómez-Hernández, J. Contam. Hydrol. **87**, 277 (2006).
[33] M. Dentz, A. Cortis, H. Scher, and B. Berkowitz, Adv. Water Resour. **27**, 155 (2004).
[34] B. Berkowitz and H. Scher, Phys. Rev. E **57**, 5858 (1998).
[35] A. F. B. Tompson, Water Resour. Res. **29**, 3709 (1993).
[36] G. S. Weissmann, Y. Zhang, E. M. LaBolle, and G. E. Fogg, Water Resour. Res. **38**, 1198 (2002).
[37] C. T. Green, Ph.D. thesis, University of California, Davis, 2002 (unpublished).
[38] P. Meakin, A. M. Tartakovsky, T. D. Scheibe, D. M. Tartakovsky, G. Redden, P. E. Long, S. C. Brooks, and Z. Xu, *Journal of Physics: Conference Series* (Institute of Physics Publishing, Bristol, United Kingdom, 2007), Vol. 78, p. 012047.
[39] A. Chechkin, V. Y. Gonchar, J. Klafter, R. Metzler, and L. V. Tanatarov, J. Stat. Phys. **115**, 1505 (2004).
[40] Y. Zhang, D. A. Benson, M. M. Meerschaert, and H.-P. Scheffler, J. Stat. Phys. **123**, 89 (2006).
[41] M. Marseguerra and A. Zoia, Ann. Nucl. Energy **33**, 1396 (2006).
[42] E. Heinsalu, M. Patriarca, I. Goychuk, G. Schmid, and P. Hanggi, Phys. Rev. E **73**, 046133 (2006).
[43] M. Magdziarz and A. Weron, Phys. Rev. E **75**, 056702 (2007).
[44] R. Schumer, D. A. Benson, M. M. Meerschaert, and B. Baeumer, Water Resour. Res. **39**, 1296 (2003).
[45] G. M. Zaslavsky, Physica D **76**, 110 (1994).
[46] M. M. Meerschaert and H.-P. Scheffler, Stochastic Proc. Appl. **118**, 1606 (2008).
[47] Y. Zhang, D. A. Benson, and B. Baeumer, Water Resour. Res. **44**, W04424 (2008).
[48] D. A. Benson and M. M. Meerschaert, http://www.stt.msu.edu/~mcubed/MRMT.pdf.
[49] S. Bochner, Proc. Natl. Acad. Sci. U.S.A. **85**, 369 (1949).
[50] W. Feller, *An Introduction to Probability Theory and Its Applications* (Wiley, New York, 1968).
[51] S. B. Yuste and K. Lindenberg, Phys. Rev. E **72**, 061103 (2005).
[52] I. M. Sokolov and R. Metzler, J. Phys. A **37**, L609 (2004).
[53] B. Baeumer and M. M. Meerschaert, Physica A **373**, 237 (2007).
[54] G. Samorodnitsky and M. S. Taqqu, *Stable Non-Gaussian Random Processes: Stochastic Models With Infinite Variance* (Chapman and Hill, New York, 1994), p. 632.
[55] M. M. Meerschaert and H.-P. Scheffler, J. Appl. Probab. **41**, 623 (2004).
[56] Y. Zhang, B. Baeumer, and D. A. Benson, Geophys. Res. Lett. **33**, L18407 (2006).
[57] T. Srokowski and A. Kaminska, Phys. Rev. E **74**, 021103 (2006).
[58] Y. Zhang, D. A. Benson, M. M. Meerschaert, E. M. LaBolle, and H. P. Scheffler, Phys. Rev. E **74**, 026706 (2006).
[59] E. E. Adams and L. W. Gelhar, Water Resour. Res. **28**, 3292 (1992).
[60] J. M. Boggs, S. C. Young, and L. M. Beard, Water Resour. Res. **28**, 3281 (1992).
[61] J. M. Boggs and E. E. Adams, Water Resour. Res. **28**, 3325 (1992).
[62] K. R. Rehfeldt, J. M. Boggs, and L. W. Gelhar, Water Resour. Res. **28**, 3309 (1992).
[63] F. J. Molz, C. Zheng, S. M. Gorelick, and C. F. Harvey, Water Resour. Res. **42**, W06603 (2006).